Energy Efficiency Optimization of IRS-Assisted UAV Networks Based on Statistical Channels

Chen Zhao, Xiaowei Pang, Weidang Lu, *Senior Member, IEEE*, Yunfei Chen, *Senior Member, IEEE*, Nan Zhao, *Senior Member, IEEE*, and Arumugam Nallanathan *Fellow, IEEE*

***Abstract*—In this letter, intelligent reflecting surface (IRS) is adopted to assist unmanned aerial vehicle (UAV) to achieve energy-efficient transmission. Specifically, the energy efficiency is maximized by jointly optimizing the UAV trajectory, transmit power and IRS phase shifts based on the statistical channel state information (CSI), since the instantaneous CSI is difficult to obtain due to the mobility of UAV and the passive structure of IRS. The non-convex problem is decomposed into two sub-problems of the trajectory and transmit power optimization, and the phase-shift optimization. To deal with the non-convexity of the first one, the successive convex approximation and Dinkelbach's algorithm are utilized. For the second one, a closed-form solution is derived directly through equivalent transformations. Then, the two sub-problems are solved iteratively to obtain an effective solution to the original problem. Simulation results are presented to validate the effectiveness of the proposed scheme.**

***Index Terms*—Energy efficiency, intelligent reflecting surface, statistical channel state information, unmanned aerial vehicle.**

I. Introduction

The applications of unmanned aerial vehicles (UAVs) in wireless communications have gained increasing attention. Benefiting from the high mobility, UAVs can be deployed rapidly compared with the conventional devices [1]. Hence, UAV communications have been widely studied in various scenarios [2]–[4]. For example, Wu *et al.* maximized the minimum throughput in a multi-UAV enabled wireless system [2]. Zhou *et al.* studied a UAV-enabled mobile edge computing wireless-powered system in [3], where the computational performance and harvested energy were both improved. For the secure transmission, Zhang *et al.* proposed two cooperative dual-UAV enabled secure data collection schemes in [4], in which the average secrecy rate and secrecy energy efficiency (EE) were maximized, respectively.

Despite of the advantages of UAVs, some users may still be in the blind areas without coverage. To resolve this issue, the technologies that enable reconfigurable propagation environments, such as holographic MIMO surfaces [5] and intelligent reflecting surface (IRS) [6], have attracted great attention. Particularly, IRS can improve the performance of UAV-aided wireless systems thanks to its ability to integrate multiple units to cooperatively generate passive beamforming [7]. In [8], Salhab and Yang investigated the applications of IRS in radio frequency and compared the IRS-equipped and IRS-aided scenarios. Huang *et al.* in [9] investigated an IRS-aided network and leveraged deep reinforcement learning (DRL) to maximize the sum rate. For the channel estimation of IRS, the works in [10] and [11] have made a detailed elaboration. Li *et al.* investigated an IRS-assisted UAV system, where the average achievable rate was maximized by optimizing the trajectory of UAV and the passive beamforming of IRS [12]. Furthermore, Mei *et al.* utilized DRL to facilitate the online decision making in UAV-IRS systems [13]. Moreover, IRS can also be mounted on UAVs as in [14] and [15], which provides a new dimension for real-time position optimization of IRS thanks to the mobility of UAV.

C. Zhao, X. Pang and N. Zhao are with the School of Information and Communication Engineering, Dalian University of Technology, Dalian 116024, China, (chiusam@mail.dlut.edu.cn, xiaoweipang00@mail.dlut.edu.cn, zhaonan@dlut.edu.cn).

W. Lu is with the College of Information Engineering, Zhejiang University of Technology, Hangzhou 310023, China (e-mail: luweid@zjut.edu.cn).

Y. Chen is with the School of Engineering, University of Warwick, Coventry CV4 7AL, U.K. (e-mail: Yunfei.Chen@warwick.ac.uk).

A. Nallanathan is with the School of Electronic Engineering and Computer Science, Queen Mary University of London, London E1 4NS, U.K. (e-mail: a.nallanathan@qmul.ac.uk).

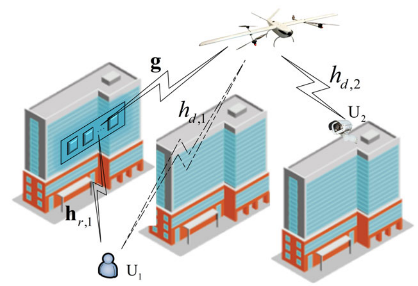

Fig. 1. IRS-assisted fixed-wing UAV air-ground network.

In the above-mentioned works, perfect instantaneous channel state information (CSI) was assumed. However, the instantaneous CSI is difficult to obtain in practice due to the mobility of UAV and the passive structure of IRS. In contrast, using statistical CSI is more practical. For instance, Gan *et al.* maximized the ergodic capacity in an IRS-assisted wireless network in both uplink and downlink in [16]. Yu *et al.* considered the simultaneous wireless information and power transfer with the aid of UAV-IRS based on the statistical CSI, where the average rate was maximized [17].

Motivated by this, we consider an IRS-aided UAV wireless network using the statistical CSI, where the UAV serves both a ground user and a high-altitude node. Considering the limited on-board energy of UAV, we aim to maximize the EE with respect to the UAV trajectory, the transmit power and the phase shifts of IRS. This problem is non-convex. Therefore, we decompose it into two sub-problems and solve them alternately through using an iterative algorithm. Numerical results show that the proposed scheme is effective to improve the EE for IRS-assisted UAV networks with statistical channels.

II. System Model

Consider an IRS-assisted air-ground network with a fixed-wing UAV as shown in Fig. 1, where the UAV serves a terrestrial user U_1 and a high-altitude node U_2 with all the nodes equipped with a single antenna. Assume that the direct path between the UAV and U_1 is blocked due to the urban dense buildings. In order to improve the strength of received signal at U_1, an IRS with M reflecting elements is deployed to establish virtual line-of-sight (LoS) channels between them.

The coordinates of U_1, U_2 and IRS are denoted as $\mathbf{q}_1 = [x_1, y_1, z_1]$, $\mathbf{q}_2 = [x_2, y_2, z_2]$ and $\mathbf{q}_I = [x_I, y_I, z_I]$, respectively. The UAV flies at a fixed altitude H with a period of T. To facilitate the analysis, T is divided into N equal time slots, i.e., $T = N\delta$, where δ is the duration of each slot. The horizontal coordinate of UAV in the n-th time slot can be denoted by $\mathbf{q}[n] = [x[n], y[n]]$, where $n \in \mathcal{N} = \{0, \ldots, N\}$. The IRS is deployed near U_1 and its passive beamforming is mainly used to assist U_1. Thus, the signal from IRS to U_2 is negligible due to the long distance. In the n-th slot, the channels from UAV to IRS and from IRS to U_1 are expressed as $\mathbf{g}[n] \in \mathbb{C}^{M\times 1}$ and $\mathbf{h}_{r,1}[n] \in \mathbb{C}^{1\times M}$, respectively, while $h_{d,k}[n]$ denotes the channel from UAV to the k-th user. Let $\mathbf{\Theta}[n] = \mathrm{diag}\{e^{j\theta_1[n]}, \ldots, e^{j\theta_M[n]}\}$ denote the phase-shift matrix of IRS in the n-th time slot, where $\theta_m[n] \in [0, 2\pi)$ is the induced phase shift of each reflecting element in the n-th time slot, $m \in \{1, \ldots, M\}$.

Due to the higher locations of both UAV and U_2, the channel between them follows the free-space path-loss model as

$$h_{d,2}[n] = \sqrt{\rho d_{U,2}^{-2}[n]}, n \in \mathcal{N}, \tag{1}$$

where ρ is the channel gain at $d_0 = 1$ m, and $d_{U,2}[n] = \|[\mathbf{q}[n], H] - \mathbf{q}_2\|$ m. Assume that the IRS is well deployed to have LoS links with both UAV and U_1. Thus, the channel cofficient between UAV and IRS can be expressed as

$$\mathbf{g}[n] = \sqrt{\rho d_{U,I}^{-2}[n]} \underbrace{\left[1, e^{-j\frac{2\pi}{\lambda}d\phi_{UI}[n]}, \ldots, e^{-j\frac{2\pi}{\lambda}(M-1)d\phi_{UI}[n]}\right]^T}_{\bar{\mathbf{g}}[n]}, \tag{2}$$

where $d_{U,I}[n] = \|[\mathbf{q}[n], H] - \mathbf{q}_I\|$, λ is the carrier wavelength, d is the antenna spacing, and $\phi_{UI}[n] = \frac{x_I - x[n]}{d_{U,I}[n]}$ represents the cosine of angle of arrival from UAV to IRS. Similarly, the channel coefficient of IRS-U_1 link can be written as

$$\mathbf{h}_{r,1} = \sqrt{\rho d_{I,1}^{-2}} \underbrace{\left[1, e^{-j\frac{2\pi}{\lambda}d\phi_{I1}}, \ldots, e^{-j\frac{2\pi}{\lambda}(M-1)d\phi_{I1}}\right]}_{\bar{\mathbf{h}}_{r,1}}, \tag{3}$$

where $d_{I,1} = \|\mathbf{q}_I - \mathbf{q}_1\|$, and $\phi_{I1} = \frac{x_1 - x_I}{d_{I,1}}$ denotes the cosine of the angle of departure from IRS to U_1.

Since U_1 is on the ground, its direct channel from UAV is usually blocked by buildings in the urban environment. Thus, we assume that U_1 is in the blind area of UAV. Then, the link from UAV to U_1 can be modeled by Rayleigh fading as

$$h_{d,1}[n] = \sqrt{\rho d_{U,1}^{-\alpha}[n]}\tilde{h}, \tag{4}$$

where α denotes the path-loss exponent, $d_{U,1}[n] = \|[\mathbf{q}[n], H] - \mathbf{q}_1\|$, and $\tilde{h}$ is a zero-mean and unit-variance circularly symmetric complex Gaussian variable.

III. Problem Formulation

Assume that the two users can access the network through orthogonal access technologies such as frequency division multiple access to avoid mutual interference. In the n-th time slot, the amount of information received by U_1 and U_2 from the UAV can be respectively expressed as

$$T_1[n] = \delta B \log_2\left(1 + \frac{P_1[n]|h_{d,1}[n] + \mathbf{h}_{r,1}\mathbf{\Theta}[n]\mathbf{g}[n]|^2}{\sigma^2}\right), \tag{5}$$

$$T_2[n] = \delta B \log_2\left(1 + \frac{P_2[n]|h_{d,2}[n]|^2}{\sigma^2}\right), \tag{6}$$

where B is the bandwidth, $P_1[n]$ and $P_2[n]$ are the transmit power for U_1 and U_2, respectively, and σ^2 is the noise power.

Referring to [18], the propulsion energy consumption of the fixed-wing UAV in the whole flight T can be given by

$$E_p = \sum_{n=1}^{N} \delta \left\{ c_1\|\mathbf{v}[n]\|^3 + \frac{c_2}{\|\mathbf{v}[n]\|}\left(1 + \frac{\|\mathbf{a}[n]\|^2 - \frac{(\mathbf{a}^T[n]\mathbf{v}[n])^2}{\|\mathbf{v}[n]\|^2}}{g^2}\right)\right\} + \frac{1}{2}\mathcal{M}\left(\|\mathbf{v}[N]\|^2 - \|\mathbf{v}[0]\|^2\right), \tag{7}$$

where c_1 and c_2 are the parameters related to UAV, $g = 9.8\ \mathrm{m/s^2}$ denotes the gravitational acceleration, $\mathcal{M}$ is the mass of UAV, $\mathbf{v}[n]$ is the velocity of the n-th time slot, with $\mathbf{v}[0]$ and $\mathbf{v}[N]$ denoting the initial and final velocities, respectively, and $\mathbf{a}[n]$ is the acceleration. The position, velocity and acceleration of UAV should satisfy

$$\mathbf{v}[n+1] = \mathbf{v}[n] + \mathbf{a}[n]\delta, n \in \{0, \ldots, N-1\}, \tag{8}$$

$$\mathbf{q}[n+1] = \mathbf{q}[n] + \mathbf{v}[n]\delta + 0.5\mathbf{a}[n]\delta^2, n \in \{0, \ldots, N-1\}, \tag{9}$$

$$\|\mathbf{v}[n]\| \le V_{max}, n \in \mathcal{N}, \tag{10}$$

$$\|\mathbf{v}[n]\| \ge V_{min}, n \in \mathcal{N}, \tag{11}$$

$$\|\mathbf{a}[n]\| \le a_{max}, n \in \mathcal{N}, \tag{12}$$

where V_{max} is the maximum speed, V_{min} is the minimum speed to guarantee the fixed-wing UAV aloft, and a_{max} is the maximum acceleration.

Another energy consumption is the transmit power, which can be given by

$$E_t = \sum_{n=1}^{N} \delta\{P_1[n] + P_2[n]\}, \tag{13}$$

and it is limited by the maximum transmit power P_{max} as

$$P_1[n] + P_2[n] \le P_{max}. \tag{14}$$

According to the above analysis, we can obtain the EE as

$$EE = \frac{\sum_{n=1}^{N}\{T_1[n] + T_2[n]\}}{E_p + E_t}. \tag{15}$$

Since the UAV keeps flying, the channels change rapidly and it is difficult to obtain the accurate CSI in real time. Thus, we are more interested in the average/expected EE based on the statistical channels, defined as $\mathbb{E}\{EE\}$. Only $T_1[n]$ involves the channel $h_{d,1}[n]$ containing random variables, which can be equivalently written as (16) at the top of the next page. To further analyze it, Proposition 1 is presented as follows.

Proposition 1: An upper bound of the amount of information can be obtained based on statistical channels such as

$$\mathbb{E}\{T_1[n]\} \le \mathbb{E}_{up}\{T_1[n]\} = \delta B \log_2\left(1 + \frac{P_1[n]}{\sigma^2}\left(\frac{X[n]}{d_{U,1}^{\alpha}[n]} + \frac{Y[n]}{d_{U,I}^{2}[n]}\right)\right), \tag{17}$$

$$\begin{aligned} T_1[n] &= \delta B \log_2\left(1+\frac{P_1[n]}{\sigma^2}\left(h_{d,1}[n]+\mathbf{h}_{r,1}\boldsymbol{\Theta}[n]\mathbf{g}[n]\right)\left(h_{d,1}[n]+\mathbf{h}_{r,1}\boldsymbol{\Theta}[n]\mathbf{g}[n]\right)^H\right) \\ &= \delta B \log_2\Bigg(1+\frac{P_1[n]}{\sigma^2}\Bigg(\underbrace{\rho d_{U,1}^{-\alpha}[n]\tilde{h}\tilde{h}^H}_{f_1}+\underbrace{2\mathrm{Re}\left\{\rho^{3/2} d_{I,1}^{-1}\overline{\mathbf{h}}_{r,1}\boldsymbol{\Theta}[n] d_{u,I}^{-1}[n]\overline{\mathbf{g}}[n] d_{U,1}^{-\alpha/2}[n]\tilde{h}^H\right\}}_{f_2}+ \\ &\quad \underbrace{\rho^2 d_{I,1}^{-2} d_{U,I}^{-2}[n]\overline{\mathbf{h}}_{r,1}\boldsymbol{\Theta}[n]\overline{\mathbf{g}}[n]\overline{\mathbf{g}}^H[n]\boldsymbol{\Theta}^H[n]\overline{\mathbf{h}}_{r,1}^H[n]}_{f_3}\Bigg)\Bigg). \end{aligned} \tag{16}$$

---

where $X[n]=\mathbb{E}\{\rho\tilde{h}\tilde{h}^H\}=\rho$ and $Y[n]=\rho^2 d_{I,1}^{-2}\overline{\mathbf{h}}_{r,1}\boldsymbol{\Theta}[n]$ $\overline{\mathbf{g}}[n]\ \overline{\mathbf{g}}^H[n]\boldsymbol{\Theta}^H[n]\overline{\mathbf{h}}_{r,1}^H$.

Proof: According to the Jensen's inequality, it holds that

$$\mathbb{E}\{\log_2(1+x)\}\le\log_2\left(1+\mathbb{E}\{x\}\right). \tag{18}$$

Applying the Jensen's inequality to (16) and referring to [16] and [17], we have

$$\begin{aligned} \mathbb{E}\{T_1[n]\}\le\mathbb{E}_{up}\{T_1[n]\}&=\delta B\log_2\left(1+\frac{P_1[n]}{\sigma^2}\mathbb{E}\left(f_1+f_2+f_3\right)\right) \\ &\overset{a}{=}\delta B\log_2\left(1+\frac{P_1[n]}{\sigma^2}\left(\frac{X[n]}{d_{U,1}^{\alpha}[n]}+\frac{Y[n]}{d_{U,I}^{2}[n]}\right)\right), \end{aligned} \tag{19}$$

where a holds because $\mathbb{E}\{f_2\}=0$ according to the statistical knowledge of $\mathbb{E}\{\tilde{h}^H\}=0$. ■

According to Proposition 1, $\mathbb{E}\{EE\}$ can be upper bounded as

$$\mathbb{E}\{EE\}\le\frac{\sum_{n=1}^{N}\left\{\mathbb{E}_{up}\{T_1[n]\}+T_2[n]\right\}}{E_p+E_t}. \tag{20}$$

We aim at maximizing the upper bound of $\mathbb{E}\{EE\}$ by jointly optimizing the UAV trajectory $\mathbf{q}[n]$, the transmit power $\mathbf{P}[n]$ and the phase shift $\boldsymbol{\Theta}[n]$, where $\mathbf{P}[n]=[P_1[n],P_2[n]]$. The problem can be formulated as

$$\text{(P1)}\quad \max_{\mathbf{q}[n],\boldsymbol{\Theta}[n],\mathbf{P}[n]}\ \frac{\sum_{n=1}^{N}\left\{\mathbb{E}_{up}\{T_1[n]\}+T_2[n]\right\}}{E_p+E_t} \tag{21a}$$

$$s.t.\ \mathbb{E}_{up}\{T_1[n]\}/\delta\ge R_{th}, n\in\{0,\ldots,N-1\}, \tag{21b}$$

$$T_2[n]/\delta\ge R_{th}, n\in\{0,\ldots,N-1\}, \tag{21c}$$

$$\mathbf{q}[0]=\mathbf{q}_B, \tag{21d}$$

$$\mathbf{q}[N]=\mathbf{q}_F, \tag{21e}$$

$$0\le\theta_m<2\pi,\forall m, \tag{21f}$$

$$(8),(9),(10),(11),(12),(14), \tag{21g}$$

where R_{th} is the rate threshold, and $\mathbf{q}_B$ and $\mathbf{q}_F$ denote the initial and final positions of UAV, respectively.

IV. Solution to Maximum Energy Efficiency

The problem (P1) is difficult to solve due to the non-convex objective function (21a) and the non-convex constraints (11), (21b) and (21c). To this end, we decompose it into two subproblems and solve them separately. Then, an iterative optimization algorithm is proposed to tackle the problem (P1).

A. Trajectory and Transmit Power Optimization

First, we optimize the trajectory and transmit power with fixed phase shifts. To deal with the non-convex constraints (21b) and (21c), we introduce two auxiliary variables $t_1[n]$ and $t_2[n]$ with

$$t_1[n]\le\log_2\left(1+\frac{P_1[n]}{\sigma^2}\left(\frac{X[n]}{u_1^{\alpha}[n]}+\frac{Y[n]}{u_I^{2}[n]}\right)\right), n\in\{0,\ldots,N-1\}, \tag{22}$$

$$t_2[n]\le\log_2\left(1+\frac{P_2[n]}{\sigma^2}\frac{\rho}{u_2^2[n]}\right), n\in\{0,\ldots,N-1\}, \tag{23}$$

where $u_1[n]$, $u_2[n]$ and $u_I[n]$ satisfy

$$d_{U,1}[n]\le u_1[n], n\in\mathcal{N}, \tag{24}$$

$$d_{U,2}[n]\le u_2[n], n\in\mathcal{N}, \tag{25}$$

$$d_{U,I}[n]\le u_I[n], n\in\mathcal{N}. \tag{26}$$

As such, the constraints (21b) and (21c) can be rewritten as

$$Bt_1[n]\ge R_{th}, n\in\{0,\ldots,N-1\}, \tag{27}$$

$$Bt_2[n]\ge R_{th}, n\in\{0,\ldots,N-1\}. \tag{28}$$

To deal with the non-convexity, we rewrite (22) and (23) as

$$\frac{\left(2^{t_1[n]}-1\right)\sigma^2}{P_1[n]}\le\frac{X[n]}{u_1^{\alpha}[n]}+\frac{Y[n]}{u_I^{2}[n]}, \tag{29}$$

$$\frac{\left(2^{t_2[n]}-1\right)\sigma^2}{P_2[n]}\le\frac{\rho}{u_2^2[n]}. \tag{30}$$

However, (29) and (30) are still non-convex due to their right sides. Specifically, $X[n]/u_1^{\alpha}[n]+Y[n]/u_I^2[n]$ and $\rho/u_2^2[n]$ are all convex differentiable functions. Note that, the first-order Taylor expansion of a convex differentiable function is its global under-estimator. Therefore, we have

$$\begin{aligned} \frac{X[n]}{u_1^{\alpha}[n]}+\frac{Y[n]}{u_I^{2}[n]}\ge{}&\frac{X[n]}{u_{1,j}^{\alpha}[n]}+\frac{Y[n]}{u_{I,j}^{2}[n]}-\alpha X[n]u_{1,j}^{-\alpha-1}[n] \\ &\left(u_1[n]-u_{1,j}[n]\right)-2Y[n]u_{I,j}^{-3}[n]\left(u_I[n]-u_{I,j}[n]\right), \end{aligned} \tag{31}$$

$$\frac{\rho}{u_2^2[n]}\ge\rho\left(\frac{3}{u_{2,j}^2[n]}-\frac{2u_2[n]}{u_{2,j}^3[n]}\right), \tag{32}$$

where $u_{1,j}[n]$, $u_{2,j}[n]$ and $u_{I,j}[n]$ are the values in the j-th iteration, and the equalities hold if and only if $u_{1,j}[n]=u_1[n]$, $u_{2,j}[n]=u_2[n]$ and $u_{I,j}[n]=u_I[n]$. Thus, we can get the new convex constraints as

$$\begin{aligned} \frac{(2^{t_1[n]}-1)\sigma^2}{P_1[n]}\le{}&\frac{X[n]}{u_{1,j}^{\alpha}[n]}+\frac{Y[n]}{u_{I,j}^{2}[n]}-\alpha X[n]u_{1,j}^{-\alpha-1}[n] \\ &(u_1[n]-u_{1,j}[n])-2Y[n]u_{I,j}^{-3}[n]\left(u_I[n]-u_{I,j}[n]\right), \end{aligned} \tag{33}$$

$$\frac{(2^{t_2[n]}-1)\sigma^2}{P_2[n]}\le\rho\left(\frac{3}{u_{2,j}^2[n]}-\frac{2u_2[n]}{u_{2,j}^3[n]}\right). \tag{34}$$

Similarly, we introduce an auxiliary variable $\tau[n]$ to deal with the non-convex constraint (11), such that

$$\tau[n]\ge V_{min}, \tag{35}$$

$$\tau[n]^2\le\|\mathbf{v}[n]\|^2, \tag{36}$$

$$\tau^2[n] \le \|\mathbf{v}_j[n]\|^2 + 2\mathbf{v}_j^T[n]\left(\mathbf{v}[n] - \mathbf{v}_j[n]\right), \tag{37}$$

where $\mathbf{v}_j[n]$ is the value obtained in the j-th iteration.

Though all the constraints have been approximated to convex ones, the problem still cannot be solved due to the non-convex objective function. We use the auxiliary variable $\tau[n]$ to decouple the velocity and acceleration in (7), and the upper bound of E_p can be obtained by

$$E_p^{up} = \sum_{n=1}^{N} \delta \left\{ c_1 \|\mathbf{v}[n]\|^3 + \frac{c_2}{\tau[n]} \left(1 + \frac{\|\mathbf{a}[n]\|^2}{g^2}\right)\right\} + \Delta k, \tag{38}$$

where $\Delta k = \frac{1}{2}\mathcal{M}\left(\|\mathbf{v}[N]\|^2 - \|\mathbf{v}[0]\|^2\right)$ denotes the change in the kinetic energy, which is related to the mass, initial speed and final speed of UAV. Without loss of generality, we assume that the initial speed is the same as the final speed, i.e., $\mathbf{v}[0] = \mathbf{v}[N]$, which means $\Delta k = 0$.

Based on the above, we can convert (P1) into (P2) as

$$\text{(P2)} \max_{\substack{\mathbf{q}[n],\mathbf{p}[n] \\ \mathbf{t}[n],\mathbf{u}_{j+1}[n],\tau[n]}} \frac{\sum_{n=1}^{N} \delta B\left\{t_1[n] + t_2[n]\right\}}{E_p^{up} + E_t} \tag{39a}$$

$$s.t. \text{ (8),(9),(10),(12),(14),(21d),(21e),(24),(25),}$$
$$\text{(26),(27),(28),(33),(34),(35),(37),} \tag{39b}$$

where $\mathbf{t}[n] = [t_1[n], t_2[n]]$ and $\mathbf{u}_j[n] = [u_{1,j}[n], u_{2,j}[n], u_{I,j}[n]]$. To deal with the fractional objective function of (P2), the Dinkelbach's method can be applied. Based on this, we define $\eta = \sum_{n=1}^{N} \delta B\left\{t_1[n] + t_2[n]\right\}$ and $\mu = E_p^{up} + E_t$, and (P2) can be transformed as

$$\text{(P3)} \max_{\substack{\mathbf{q}[n],\mathbf{p}[n] \\ \mathbf{t}[n],\mathbf{u}[n],\tau[n]}} \eta - \gamma\mu \tag{40a}$$

$$s.t. \text{ (8),(9),(10),(12),(14),(21d),(21e),(24),(25),}$$
$$\text{(26),(27),(28),(33),(34),(35),(37),} \tag{40b}$$

where γ is a coefficient related to η and μ. Thus, (P3) is convex and can be solved via CVX.

B. Phase-Shift Optimization

We optimize the phase shifts based on the obtained trajectory and transmit power. According to (5) and (6), the phase shifts of IRS only affects the throughput of U_1, i.e., $\mathbb{E}_{up}\{T_1[n]\}$[1]. The problem can be formulated as

$$\text{(P4)} \max_{\boldsymbol{\Theta}[n]} \mathbb{E}_{up}\{T_1[n]\} \tag{41a}$$

$$s.t. \ 0 \le \theta_m[n] < 2\pi, \forall m. \tag{41b}$$

According to (19), $P_1[n]/\sigma^2$ and $X[n]/d_{U,1}^{\alpha}[n]$ are the constants when the trajectory and transmit power are fixed. Thus, the objective function (41a) can be approximated to maximizing $Y[n]/d_{U,I}^2[n]$, which is equivalent to maximizing $|\mathbf{h}_{r,1}^H\boldsymbol{\Theta}[n]\mathbf{g}[n]|$. Although it is still a non-convex optimization problem, we can get a closed-form solution due to its special form. Specifically, we can establish

$$|\mathbf{h}_{r,1}^H\boldsymbol{\Theta}[n]\mathbf{g}[n]| = \left|\boldsymbol{\theta}[n]\mathrm{diag}\{\mathbf{h}_{\mathrm{r},1}^{\mathrm{H}}\}\mathbf{g}[n]\right|, \tag{42}$$

[1]Note that it can be easily extended to the multi-user scenarios where the IRS serves different users in different time slots, using the same optimization algorithm.

where $\boldsymbol{\theta}[n] = \{e^{j\theta_1[n]}, \dots, e^{j\theta_M[n]}\}$. Thus, the right side of (42) in element-wise can be expressed as

$$\begin{aligned}
&\left|\left[e^{j\theta_1[n]}, \dots, e^{j\theta_M[n]}\right]\begin{bmatrix} h_{r,1,1}^H & & \\ & \ddots & \\ & & h_{r,1,M}^H\end{bmatrix}\begin{bmatrix} g_1[n] \\ \vdots \\ g_M[n]\end{bmatrix}\right| \\
&= \left|e^{j\theta_1[n]}h_{r,1,1}^H g_1[n] + \dots + e^{j\theta_M[n]}h_{r,1,M}^H g_M[n]\right| \\
&\overset{(b)}{\le} \left|e^{j\theta_1[n]}h_{r,1,1}^H g_1[n]\right| + \dots + \left|e^{j\theta_M[n]}h_{r,1,M}^H g_M[n]\right|,
\end{aligned} \tag{43}$$

where the equality at (b) holds if and only if $\arg(e^{j\theta_1[n]}h_{r,1,1}^H g_1[n]) = \dots = \arg(e^{j\theta_M[n]}h_{r,1,M}^H g_M[n]) = \theta^*$, i.e., the angle of each item is the same. Without loss of generality, assume $\theta^* = 0$. Therefore, the phase shift of the m-th element of IRS in the n-th slot can be denoted as

$$\theta_m[n] = -\arg\left(h_{r,1,m}^H g_m[n]\right). \tag{44}$$

Based on the above, the two sub-problems can be solved separately. To solve the original problem (P1), we propose an iterative algorithm summarized in Algorithm 1. The total computational complexity of this algorithm is $\mathcal{O}(I_{out}(I_{in}(5N + 3KN)^{3.5}))$, where I_{out} and I_{in} are the numbers of the outer loop and inner loop, respectively.

Algorithm 1 Iterative algorithm for (P1)

Initialize $\mathbf{q}$ and $\boldsymbol{\Theta}$.
Repeat
  Set $\gamma = 1$ and the number of iteration $j = 1$. Based on the trajectory $\mathbf{q}$, get $\mathbf{v}_j[n]$, $u_{1,j}[n]$, $u_{2,j}[n]$ and $u_{I,j}[n]$.
  Repeat
    Solve (P3) with given $\{\gamma, \mathbf{v}_j[n], u_{1,j}[n], u_{2,j}[n], u_{I,j}[n], \boldsymbol{\Theta}\}$ to get $\{\mathbf{v}_{j+1}[n], u_{1,j+1}[n], u_{2,j+1}[n], u_{I,j+1}[n]\}$.
    Update: $j = j + 1$, $\gamma = \eta/\mu$.
  Until Convergence and obtain $\mathbf{q}$
  Get $\boldsymbol{\Theta}$ with $\mathbf{q}$ in the closed form.
Until Convergence and obtain EE

V. Simulation Results and Discussion

Simulation results are provided to evaluate the performance of the proposed algorithm. Unless otherwise specified, the parameters are listed as follows. The flight altitude and period of UAV are 100 m and 50 s, respectively. The parameters of UAV are set to $c_1 = 9.26 \times 10^{-4}$, $c_2 = 2250$, $V_{max} = 100$ m/s, $V_{min} = 10$ m/s , $a_{max} = 5$ m/s^2, and $\delta = 0.2$ s [18]. The positions are set to $\mathbf{q}_1 = [200 \ -400 \ 0]$ m, $\mathbf{q}_2 = [700 \ -300 \ 50]$ m, $\mathbf{q}_I = [195 \ -400 \ 20]$ m, $\mathbf{q}_B = [0 \ 0]$ m and $\mathbf{q}_F = [1000 \ 0]$ m. The number of IRS reflecting elements M is 25. The channel gain at unit distance is set to $\rho = -30$ dB, the path-loss exponent $\alpha = 3.5$ and the noise power is set as $\sigma^2 = -110$ dBm. The maximum transmit power is 0.3 W, the bandwidth for each user is 360 KHz and the rate is no less than 2 Mbit/s.

Fig. 2 shows the trajectories of UAV with different flight periods and user distributions. Specifically, taking the line between the start and ending positions of UAV as a reference, the users are distributed on the same side in Fig. 2 (a) and on different sides in Fig. 2 (b). Note that Fig. 2 is horizontal without showing the heights. The positions of U_1 and IRS in

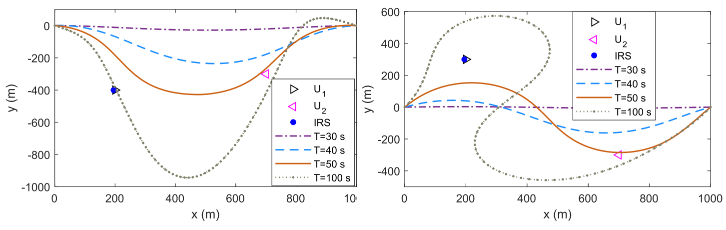

(a) On one side (b) On both sides

Fig. 2. Trajectories of UAV with different flight periods and user distributions.

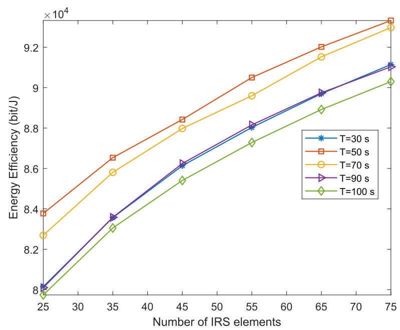

Fig. 3. Energy efficiency versus the number of IRS elements.

Fig. 2 (b) are [200 300 0] m and [195 300 20] m, respectively. We can see from Fig. 2 that when the period is small, the trajectory of UAV is close to a straight line due to the initial and final positions. While as the period increases, the UAV adjusts its trajectory according to different user distributions to get closer to the users. However, since the fixed-wing UAV cannot hover over the users and requires a certain speed to stay aloft, the UAV will move away from users if the period is relatively large, e.g., $T = 100$ s.

Fig. 3 shows the EE versus the number of IRS reflecting elements. We can observe that the EE increases with the number of IRS elements. This is because a larger IRS can achieve higher passive beamforming gain to enhance the received signal power at U_1, and the EE can be improved. We can also observe that a higher T results in an enhancement in EE when $T \leq 50$ s. However, when $T \geq 70$ s, increasing T leads to a decreased EE. This can be attributed to the observations in Fig. 2, where the UAV would fly away from users over a relatively large period.

In Fig. 4, we compare the proposed scheme (PS) with other benchmarks, namely without power optimization (W-PO), without phase-shift optimization (WPSO) and without trajectory optimization (WTO). We plot the EE, the amount of information and the energy consumption in one flight period of the four schemes for comparison. We can see that the overall EE of the proposed scheme is always the highest. This is because Algorithm 1 will make a trade-off between the amount of information and the energy consumption to meet the service requirement, while maximizing the EE.

VI. Conclusions

In this letter, we proposed an energy-efficient IRS-assisted UAV transmission scheme based on the statistical CSI. The ergodic EE was maximized by optimizing the UAV trajectory, the transmit power, and the IRS phase shifts. We first transformed the original non-convex problem into two sub-problems and approximated them as convex ones, and then iteratively solved the two sub-problems to obtain a feasible solution to the original one. We derived a design based on the statistical CSI to avoid the challenging real-time channel acquisition, and simulation results show that the proposed scheme is effective in improving the EE.

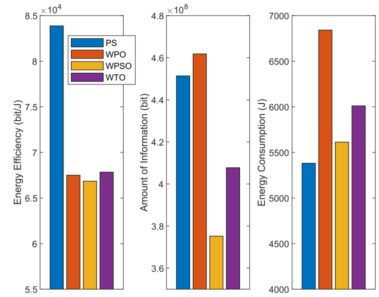

Fig. 4. Energy efficiency, amount of information and energy consumption of four schemes.

References

[1] Y. Zeng, R. Zhang, and T. J. Lim, "Wireless communications with unmanned aerial vehicles: Opportunities and challenges," *IEEE Commun. Mag.*, vol. 54, no. 5, pp. 36–42, May 2016.

[2] Q. Wu, Y. Zeng, and R. Zhang, "Joint trajectory and communication design for multi-UAV enabled wireless networks," *IEEE Trans. Wireless Commun.*, vol. 17, no. 3, pp. 2109–2121, Jan. 2018.

[3] F. Zhou, Y. Wu, R. Q. Hu, and Y. Qian, "Computation rate maximization in UAV-enabled wireless-powered mobile-edge computing systems," *IEEE J. Sel. Area. Comm.*, vol. 36, no. 9, pp. 1927–1941, Aug. 2018.

[4] R. Zhang, X. Pang, W. Lu, N. Zhao, Y. Chen, and D. Niyato, "Dual-UAV enabled secure data collection with propulsion limitation," *IEEE Trans. Wireless Commun.*, vol. 20, no. 11, pp. 7445–7459, Jun. 2021.

[5] C. Huang *et al.*, "Holographic MIMO surfaces for 6G wireless networks: Opportunities, challenges, and trends," *IEEE Wireless Commun.*, vol. 27, no. 5, pp. 118–125, Jul. 2020.

[6] Q. Wu and R. Zhang, "Towards smart and reconfigurable environment: Intelligent reflecting surface aided wireless network," *IEEE Commun. Mag.*, vol. 58, no. 1, pp. 106–112, Jan. 2020.

[7] X. Pang *et al.*, "When UAV meets IRS: Expanding air-ground networks via passive reflection," *IEEE Wireless Commun.*, vol. 28, no. 5, pp. 164–170, Oct. 2021.

[8] A. M. Salhab and L. Yang, "Mixed RF/FSO relay networks: RIS-equipped RF source vs RIS-aided RF source," *IEEE Wireless Commun. Lett.*, vol. 10, no. 8, pp. 1712–1716, May 2021.

[9] C. Huang *et al.*, "Reconfigurable intelligent surface assisted multiuser MISO systems exploiting deep reinforcement learning," *IEEE J. Sel. Area. Comm.*, vol. 38, no. 8, pp. 4640–4655, Aug. 2020.

[10] W. Li *et al.*, "Multi-user holographic MIMO surfaces: Channel modeling and spectral efficiency analysis," *IEEE J. Sel. Top. Signal Process.*, vol. 16, no. 5, pp. 1112–1124, May 2022.

[11] W. Li *et al.*, "Joint channel estimation and signal recovery for RIS-empowered multiuser communications," *IEEE Trans. Commun.*, vol. 70, no. 7, pp. 4640–4655, Jun. 2022.

[12] S. Li *et al.*, "Reconfigurable intelligent surface assisted UAV communication: Joint trajectory design and passive beamforming," *IEEE Wireless Commun. Lett.*, vol. 9, no. 5, pp. 716–720, May 2020.

[13] H. Mei *et al.*, "3D-trajectory and phase-shift design for RIS-assisted UAV systems using deep reinforcement learning," *IEEE Trans. Veh. Technol.*, vol. 71, no. 3, pp. 3020–3029, Jan. 2022.

[14] M. Al-Jarrah *et al.*, "Capacity analysis of IRS-based UAV communications with imperfect phase compensation," *IEEE Wireless Commun. Lett.*, vol. 10, no. 7, pp. 1479–1483, Jul. 2021.

[15] X. Song, Y. Zhao, Z. Wu, Z. Yang, and J. Tang, "Joint trajectory and communication design for IRS-assisted UAV networks," *IEEE Wireless Commun. Lett.*, vol. 11, no. 7, pp. 1538–1542, May 2022.

[16] X. Gan, C. Zhong, C. Huang, and Z. Zhang, "RIS-assisted multi-user MISO communications exploiting statistical CSI," *IEEE Trans. Commun.*, vol. 69, no. 10, pp. 6781–6792, Oct. 2021.

[17] K. Yu, X. Yu, and J. Cai, "UAVs assisted intelligent reflecting surfaces SWIPT system with statistical CSI," *IEEE J. Sel. Top. Signal Process.*, vol. 15, no. 5, pp. 1095–1109, Aug. 2021.

[18] Y. Zeng and R. Zhang, "Energy-efficient UAV communication with trajectory optimization," *IEEE Trans. Wireless Commun.*, vol. 16, no. 6, pp. 3747–3760, Jun. 2017.